

Surface enhancement in near-field Raman spectroscopy

E. J. Ayars and H. D. Hallen^{a)}

Physics Department, North Carolina State University, Raleigh, North Carolina 27695-8202

(Received 25 February 2000; accepted for publication 5 May 2000)

The intensity and selection rules of Raman spectra change as a metal surface approaches the sample. We study the distance dependence of the new Raman modes with a near-field scanning optical microscope (NSOM). The metal-coated NSOM probe provides localized illumination of a metal surface with good distance control. Spectra are measured as the probe approaches the surface, and the changes elucidated with difference spectra. Comparisons to a theoretical model for Raman excitation by evanescent light near the probe tip indicate that while the general trends are well described, the data show oscillations about the model. © 2000 American Institute of Physics. [S0003-6951(00)04326-6]

The proximity of sharp metallic structures to a sample has profound effects on the Raman spectra of that sample. It leads to surface enhanced Raman spectroscopy, for example see Refs. 1 and 2, and references within, and to differences between far-field and near-field Raman spectroscopy measured with a near-field optical microscope (NSOM).³⁻⁶ Two aspects of the spectra, the selection rules and the mode intensities, are altered by the presence of the metal. We concentrate in this letter on the dependence of the intensity of the new modes with distance between the metal-coated probe and the dielectric surface. This enhancement originates from the evanescent light present near the probe tip. A model describing the fields near such a small aperture was described by Bethe⁷ and later modified by Bouwkamp.⁸ Betzig and Chichester⁹ measured the fields near a NSOM tip using single fluorescent molecules as detectors and found good agreement with this theory. We show in this letter that the theory can also explain the general trends of the experimental enhancements in Raman spectroscopy, but that the data show oscillations about the theoretical curve as the tip approaches the surface.

Near-field scanning optical microscopy (NSOM)¹⁰ provides a unique method to study the effects of metal in proximity to the sample under Raman scrutiny. The aluminum-coated probe, forming the NSOM aperture, can be moved with nanometer accuracy to and from the surface. Force feedback of the NSOM is used as an indicator of distance,^{11,12,13} in combination with a calibrated piezoelectric scanner. A cooled ($-45\text{ }^{\circ}\text{C}$) charge coupled device (CCD) camera in the photon counting mode is used in conjunction with a Jarrel-Ash Czerney-Turner spectrometer for the Raman signal detection. An argon ion laser operating at 514.5 nm provides the excitation. In this experiment, the sample is illuminated through a tapered fiber probe, which is mounted through the center of a 0.5 numerical aperture aspheric lens. The backscattered light from the sample is collected and collimated with this lens. The light then passes through a holographic notch filter to remove elastically scattered light before being focused into the spectrometer. The primary difficulty encountered in NSOM Raman is that of low signal

levels. This cannot be countered by increased input intensity, as input of more than a few milliwatts of light into the back of the fiber will destroy the probe tip.¹⁴ Smaller tip apertures strongly reduce the probe throughput,¹⁵ and Raman cross sections are relatively small. Care was taken in the design and thermal isolation of the microscope so that it would be stable,^{16,17} since low signal levels necessitate long integration times.

The material studied here is KTiOPO_4 (KTP), a nonlinear optical material used for second harmonic generation. After a coarse approach to the surface, the probe tip was brought towards the surface until the force feedback signal indicated contact. A Raman spectrum and background were taken for reproducibility verification. The tip was then pulled back by again changing the feedback value until the tip was as far from the surface as feedback would allow. Raman spectra were acquired at approximately 10 min intervals, averaging in each case for 5 min. Between scans, the feedback level was adjusted until the tip-sample distance was reduced by the desired amount, between 4 and 12 nm, depending upon the distance from the surface. The final scan (in contact once more) was compared with the original to verify that any observed changes did not originate from damage to the tip.

Since the microscope is well isolated from the environment, the primary cause of drift is piezoelectric creep. We therefore fit the change in the feedback position during spectra acquisition to an exponential decay. The fit is quite good, and indicates that the piezoelectric creep decays with a 24 min time constant. Thus, the positions of the first few spectra had to be adjusted to account for the creep. The correction factors are small for the others, and the distances the piezoelectric moves between spectra are accurate measures of the probe-sample distance change between the spectra. Problems again arise when the probe-sample interaction becomes strong at very small distances. Large piezoexcursions are observed for small feedback level changes. It is likely that the probe is now pushing into the surface and deforming the surface so that the actual probe sample distance change is small. Since the probe approaches the surface at a slight angle, only one corner will touch first, so although the distance variation is reduced, it is not 0. In the figures, we arbitrarily set the distance values for the final two spectra,

^{a)}Electronic mail: hans_Hallen@ncsu.edu

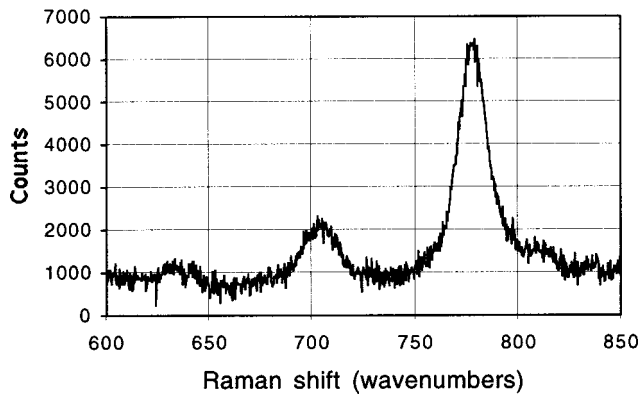


FIG. 1. A NSOM-Raman spectrum taken with the probe nearly in contact with the surface. A background "dark" spectrum for the CCD has been subtracted. The integration time for this spectrum was 5 min.

closest to the surface, as 0 and 1 nm, to avoid unnecessarily skewing the distance scale due to this effect.

One of these final spectra, after subtraction of the CCD background, is shown in Fig. 1. The general shape is typical of all the spectra in the series. This region of the Raman spectrum contains vibrations primarily from TiO_6 stretching modes in the KTP. The largest peak, centered at 778 cm^{-1} , has a width at half height of 18 cm^{-1} . This is likely the strong totally symmetric A1 vibration mode, which has been observed before in both near- and far-field measurements.^{4-6,18,19} The next-largest peak, centered at 706 cm^{-1} , has a width at half height of 19 cm^{-1} . This could be the 699 cm^{-1} B1, the 701 cm^{-1} B2, or the 695 cm^{-1} A2 vibration. This peak is strong even when the probe is retracted from the surface, which precludes vibrations of the antisymmetric B1 and B2 symmetry, so it is most likely the A2 mode. A smaller shoulder is observed at an energy slightly higher than the largest peak, $\sim 810\text{--}812 \text{ cm}^{-1}$. We have not found a reference to a line at an energy this high. This and the smaller 640 cm^{-1} line do not have sufficient signal in the comparative spectra to overcome the noise, so we ignore them.

The changes observed as the probe approaches the surface are rather small, so we resort to comparative spectra. Several spectra taken far from the surface were averaged, to improve signal-to-noise, and subtracted from single spectrum acquired closer to the surface. The results are shown in Fig. 2. The two existing peaks do not grow as the probe approaches the surface. They should not, since the lateral fields are not significantly enhanced near the probe. New peaks arise in the comparative spectra, at higher energies than their far-field counterparts. In particular, the bigger peak centered at 787 cm^{-1} has a width at half height of 18 cm^{-1} . The smaller peak centered at 712 cm^{-1} has a width at half height of $\sim 20 \text{ cm}^{-1}$. This big peak can be attributed to the B1 peak at 783 cm^{-1} reported previously.¹⁹ The B1 symmetry requires a polarization component in the z direction, normal to the surface. An electric field in the z direction exists near the metal probe tip so that the metal boundary conditions are satisfied, but does not exist away from the probe. Thus, the B1 vibration cross section should be enhanced according to the local strength of the z -polarized electric field and should not be observed in the NSOM far field.

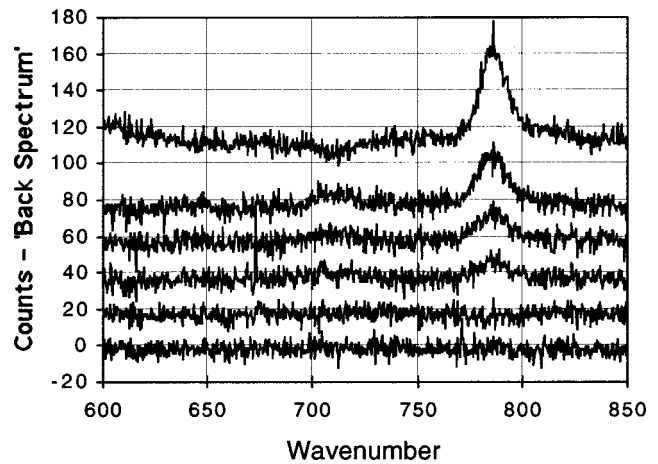


FIG. 2. Several difference spectra generated by subtracting an average of several spectra with the probe far from the surface from a Raman spectrum at the distance noted later. The integration time for all spectra was 5 min. The spectra are shifted by 20 from each other for clarity. From the top to the bottom: (a) in contact, (b) close to contact (this is the difference spectrum corresponding to the spectrum shown in Fig. 2), (c) 47 nm further than (b), (d) 70 nm from (b), (e) 108 nm, and (f) 127 nm.

A quantitative comparison with the Bethe-Bouwkamp theory is shown in Fig. 3. The points with error bars result from integrating the area under the large or the small peaks and subtracting the average background calculated from regions on either side of each peak. The two integrals are plotted on different scales so a comparison of the variations can be made. The theory line, solid, is the integral at a constant z value of the squared, numerically calculated electric field in the z direction. It assumes an aperture size of 200 nm and has been multiplied by an arbitrary scale factor. The aperture size chosen is not critical, as a change to the aperture size can be

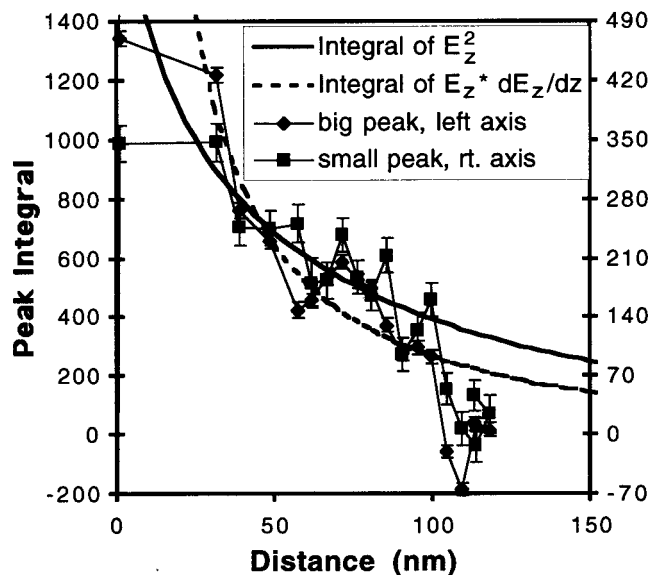


FIG. 3. The integral of the peaks in Fig. 2 as a function of probe-sample distance is shown with error bars. The two are plotted on different scales so that the dependence on distance can be compared. Several values are averaged on either side of the peak to calculate the background, which is subtracted. The solid line results from a numerical calculation of the electric field in the direction normal to the surface squared. The field squared is integrated over the plane at each distance, and the result scaled to approximately match the data. The electric field times its gradient calculated with the same model is also shown.

counteracted by an adjustment of the scale factor. The general trend of the data is captured well by the model, although the data show oscillations, which will be discussed later.

The explanation of the smaller, 712 cm^{-1} , peak is not as straightforward, since there are no Raman lines previously observed that are strong enough, even considering alternative polarization states. Most studies have not reported any line at this energy, although Kugel *et al.*¹⁸ have reported an extremely weak peak in the B1 geometry at 716 cm^{-1} . Such a line would have the same symmetry as that in the discussion earlier, although the above 783 cm^{-1} line is found in many studies and is reported as “strong,” a criterion common to many of the lines observed in the signal-starved NSOM Raman. A fairly strong peak at 716 cm^{-1} has previously been observed in NSOM Raman with the probe close to the surface,^{3,4} but no distance dependent measurements were made. This peak can be explained²⁰ by the coupling through the electric field gradient to the strong infrared (IR) absorption line at 712 cm^{-1} .²¹ The selection rules for the gradient field Raman (GFR) are similar to those for IR absorption and signal levels in the near field are predicted to be similar to Raman intensities, so this effect would provide a strong peak at the correct energy. The electric field gradient is strong near the metal surface, i.e., near the probe, and decreases away from the metal. Therefore it should follow the same trends as the data. We used the Bethe–Bouwkamp model to calculate the integral of the z component of the electric field, E_z , times the derivative of E_z with respect to z , dE_z/dz . This is the factor in GFR that takes the place of E^2 in spontaneous Raman spectroscopy. It is shown after scaling as a dotted line in Fig. 3. The similarity between the two scaled theory lines results from the nearly exponential decay of the evanescent z -polarized light with distance from the metal.

The data in Fig. 3 do not fall upon a smooth line, but rather show oscillations about the smooth line that are large compared to the error. The agreement between the data from the two peaks supports the common origin of this phenomenon. One of the oscillations causes the data from the big peak to drop below 0—the value of that peak integral actually decreased as the probe approached the surface. This is not an artifact due to the background estimate. An examination of the difference spectra that is second from the bottom in Fig. 2 shows a clear dip rather than a peak at the same energy as the big peak. The magnitude of the oscillations is not very clean, although one can identify a $\sim 20\text{ nm}$ period component at larger distances, which lengthens as the probe approaches the surface. The origin of these oscillations remains unknown. The length scale is too long for a description in terms of Fermi oscillations. The length scale is too short for optical interference or diffraction mechanisms. We are not operating near any plasma resonances of aluminum. If the substrate were a metal, waveguide mode cutoff effects could be important in the reflection geometry, but the dielectric substrate should not form a strong waveguide with the tip.

In addition to the oscillations, the measured peak integral data fall below the model when the probe nears the surface. As noted earlier, it is likely that the probe may be contacting and deflecting the surface, thus reducing the distance change. We have no way to measure this phenomenon, but it would cause a shift in those points to the left, as is apparently the case for the last few points. This pressure on the surface is most obvious in the spectrum closest to the surface, the top-most spectrum in Fig. 2. The big peak is much bigger than would be expected by an extrapolation of the other data (its integral is 2373), and the small peak integral is negative (-283), again not what would be expected from extrapolation in Fig. 3.

In summary, we have measured the changes in Raman spectra intensity as a metal probe approaches a surface. General trends are described well by a simple model for the electric fields near a metal-coated NSOM probe. Two different vibration modes are tracked and show similar dependence on probe-sample distance. Oscillations of the data about the model are found, but remain unexplained.

The authors thank Catherine Jahncke, Suzanne Huerth, Michael Taylor, and Steve Winder for useful discussions or assistance. This work was supported by the U.S. Army Research Office through Grant No. DAAH04-93-G-0194, the Office of Naval Research through Grant No. N00014-98-1-0228, and the National Science Foundation through Grant No. DMR-9975543.

¹M. Moskovits, *Rev. Mod. Phys.* **57**, 783 (1985).

²J. A. Creighton, in *Spectroscopy of Surfaces*, edited by R. J. H. Clark and R. E. Hester (Wiley, New York, 1988), p. 37.

³H. D. Hallen, A. H. La Rosa, and C. L. Jahncke, *Phys. Status Solidi A* **152**, 257 (1995).

⁴C. L. Jahncke, M. A. Paesler, and H. D. Hallen, *Appl. Phys. Lett.* **67**, 2483 (1995).

⁵C. L. Jahncke, H. D. Hallen, and M. A. Paesler, *J. Raman Spectrosc.* **27**, 579 (1996).

⁶C. L. Jahncke and H. D. Hallen, *Proceedings of 9th annual meeting of IEEE Lasers and Electro-Optics Society (LEOS)* 96 (1996), Vol. 1, p. 176.

⁷H. A. Bethe, *Phys. Rev.* **66**, 163 (1944).

⁸C. J. Bouwkamp, *Philips Res. Rep.* **5**, 401 (1950).

⁹E. Betzig and R. J. Chichester, *Science* **262**, 1422 (1993).

¹⁰E. Betzig and J. K. Trautman, *Science* **257**, 189 (1992).

¹¹E. Betzig, P. L. Finn, and J. S. Weiner, *Appl. Phys. Lett.* **60**, 2484 (1992).

¹²R. Toledo-Crow, P. C. Yang, Y. Chen, and M. Vaez-Iravani, *Appl. Phys. Lett.* **60**, 2957 (1992).

¹³K. Karrai and R. D. Grober, *Appl. Phys. Lett.* **66**, 1842 (1995).

¹⁴A. H. LaRosa, B. I. Yakobson, and H. D. Hallen, *Appl. Phys. Lett.* **67**, 2597 (1995).

¹⁵B. I. Yakobson and M. A. Paesler, *Ultramicroscopy* **57**, 204 (1995).

¹⁶C. L. Jahncke and H. D. Hallen, *Rev. Sci. Instrum.* **68**, 1759 (1997).

¹⁷E. J. Ayars and H. D. Hallen (unpublished).

¹⁸G. E. Kugel, F. Brehat, B. Wyncke, M. D. Fontana, G. Marnier, C. Carabatos-Nedelec, and J. Mangin, *J. Phys. C* **21**, 5565 (1988).

¹⁹H.-G. Yang, B.-Y. Gu, Y.-Y. Wang, H. Cheng-en, and De-Z. Shen, *Guangxue Xuebao* **6**, 1071 (1986).

²⁰E. J. Ayars, H. D. Hallen, and C. L. Jahncke (unpublished).

²¹J. C. Jacco, *Mater. Res. Bull.* **21**, 1189 (1986).